Molecular Crystals and Liquid Crystals

Publication details, including instructions for authors and subscription information:
http://www.tandfonline.com/loi/gmcl20

Local Alignment Order in Isotropic Structure of Hard Spherical Discs

Tomonori Koda [a], Akihiro Nishioka [a] & Susumu Ikeda [a]

[a] Faculty of Engineering, Yamagata University, Jonan, Yonezawa, Japan

Version of record first published: 17 Oct 2011

To cite this article: Tomonori Koda, Akihiro Nishioka & Susumu Ikeda (2005): Local Alignment Order in Isotropic Structure of Hard Spherical Discs, Molecular Crystals and Liquid Crystals, 441:1, 339-348

To link to this article: http://dx.doi.org/10.1080/154214091010057

Mol. Cryst. Liq. Cryst., Vol. 441, pp. 339–348, 2005

ISSN: 1542-1406 print/1563-5287 online
DOI: 10.1080/154214091010057

Taylor & Francis
Taylor & Francis Group

Local Alignment Order in Isotropic Structure of Hard Spherical Discs

Tomonori Koda
Akihiro Nishioka
Susumu Ikeda
Faculty of Engineering, Yamagata University, Jonan, Yonezawa, Japan

We performed isobaric Monte Carlo simulation of hard disc-like particles called spherical discs. Shape of spherical discs is determined by a sweep of the center of sphere of radius L on a disc of radius D. Simulations of pressure decreasing and increasing processes of 480 spherical discs of $D/L = 5$ indicated that ordered phase of hexagonal columns of discs melted into isotropic phase without showing nematic structure. Results indicate that local column structure continuously grows in global isotropic structure.

I. INTRODUCTION

Computer simulations have shown that hard anisotropic model molecules show various types of liquid crystal structures. Nematic structure is observed in systems of hard spherocylinders [1–4], cut spheres [5,6], and hard ellipsoids of revolution [7]. Columnar structure is observed for cut spheres [5,6]. Smectic structure is observed in systems of hard spherocylinders [1–4].

If we categorize shapes of model molecules into rod-like molecules and disc-like molecules, spherocylinders are grouped as rod-like, cut spheres are disc-like, and group of ellipsoids of revolution depends on aspect ratio of symmetry axes. In this study we present simulation results for another type of disc-like model molecule called spherical disc [8].

This work was supported by Grants-in-Aid from the Ministry of Education, Culture, Sports, Science and Technology of Japan, No. 15607002 and 15300250. Support by Aomori Prefecture Collaboration of Regional Entities for the Advancement of Technological Excellence, JST is also gratefully acknowledged.

Address correspondence to Tomonori Koda, Faculty of Engineering, Yamagata University, 4-3-16 Jonan, Yonezawa 992-8510, Japan. E-mail: koda@yz.yamagata-u.ac.jp

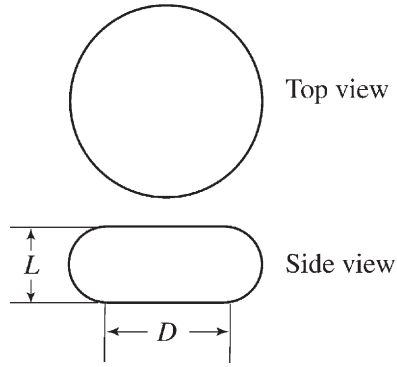

FIGURE 1 Shape of spherical disc.

II. MOLECULAR MODEL

Spherocylinder is a cylinder each end of which is capped with a hemisphere. Its shape is determined by a sweep of the center of a sphere on a line segment. The spherical disc is an extension of spherocylinder to a disc-like molecule. The shape is described by Figure 1. It is determined by a sweep of the center of sphere of diameter L on the core disc of diameter D. Volume of one spherical disc v_0 is given by

$$v_0 = \frac{\pi}{4}\left[\frac{2}{3}L^3 + \frac{\pi}{2}DL^2 + D^2L\right]. \tag{1}$$

Monte Carlo (MC) simulation generates molecular configurations avoiding molecular overlap. Two spherical discs overlap each other when minimum distance between core discs of diameter D is smaller than L.

As Figure 2 shows, there are three cases for minimum distance between two core discs. For the case of Figure 2(a), two discs overlap

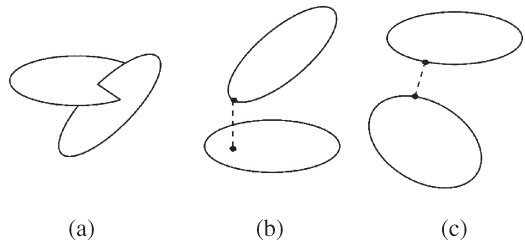

FIGURE 2 Three cases for minimum distance between two core discs.

each other. In the case of Figure 2(b), the minimum distance is provided by a point on body of one disc and a point on circumference of the other. Figure 2(c) corresponds to the case in which the minimum distance is between points on circumferences of two discs. Analytical calculation of the minimum distance is possible for the cases (a) and (b) of Figure 2, however, for the case (c), we needed numerical search to obtain the minimum distance.

For convenience, we denote the core disc of k-th spherical disc as k-th core disc. When two core discs are in the case (c) of Figure 2, we set a base for the numerical search on one of core discs. In the case of Figure 3 , the base is set on the k-th core disc.

Let us denote a vector running from a point P to a point Q as $\overrightarrow{PQ}$. When a point B gives a minimum distance between a point A on the circumference of k-th core disc to the circumference of j-th core disc, $\overrightarrow{O_jB}$ is on a plane determined by $\overrightarrow{O_jA}$ and $\boldsymbol{n}_j$, where as described by Figure 3, O_j is the center of j-th core disc and $\boldsymbol{n}_j$ is the normal of j-th disc. The point B satisfies

$$\overrightarrow{O_jB} = \frac{r_j(\boldsymbol{n}_j \times \overrightarrow{O_jA}) \times \boldsymbol{n}_j}{\left|(\boldsymbol{n}_j \times \overrightarrow{O_jA}) \times \boldsymbol{n}_j\right|}, \tag{2}$$

where r_j is radius of j-th core disc, and $\boldsymbol{a} \times \boldsymbol{b}$ is vector product made by $\boldsymbol{a}$ and $\boldsymbol{b}$. Vector running from A to B is given by

$$\begin{aligned} \overrightarrow{BA} &= \overrightarrow{O_jA} - \overrightarrow{O_jB}, \\ &= \boldsymbol{R}_{kj} + \boldsymbol{r}_A - \frac{r_j\{\boldsymbol{R}_{kj} + \boldsymbol{r}_A - [(\boldsymbol{R}_{kj} + \boldsymbol{r}_A) \cdot \boldsymbol{n}_j] \cdot \boldsymbol{n}_j\}}{|\boldsymbol{R}_{kj} + \boldsymbol{r}_A - [(\boldsymbol{R}_{kj} + \boldsymbol{r}_A) \cdot \boldsymbol{n}_j]\boldsymbol{n}_j|}, \end{aligned} \tag{3}$$

where $\boldsymbol{R}_{kj} = \overrightarrow{O_jO_k}$, $\boldsymbol{r}_A = \overrightarrow{O_kA}$, and $\boldsymbol{a} \cdot \boldsymbol{b}$ expresses scalar product made by vectors $\boldsymbol{a}$ and $\boldsymbol{b}$. We denote square of $|\overrightarrow{BA}|$ by ξ that is expressed as

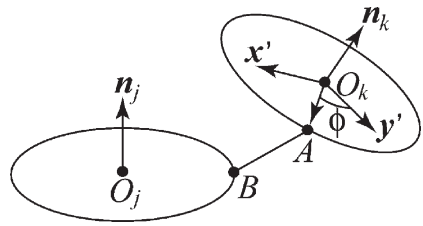

FIGURE 3 Base on k-th disc for numerical search of minimum distance between j-th and k-th disc.

$$\begin{aligned}\xi &= \overrightarrow{BA} \cdot \overrightarrow{BA} \\ &= \boldsymbol{R}_{kj} \cdot \boldsymbol{R}_{kj} + r_k^2 + r_j^2 + 2\boldsymbol{R}_{kj} \cdot \boldsymbol{r}_A \\ &\quad - 2r_j\sqrt{(\boldsymbol{R}_{kj} + \boldsymbol{r}_A)^2 - [(\boldsymbol{R}_{kj} + \boldsymbol{r}_A) \cdot \boldsymbol{n}_j]^2}.\end{aligned} \tag{4}$$

Differential of ξ due to differential of $\boldsymbol{r}_A$ is expressed as

$$d\xi = \left\{ 2\boldsymbol{R}_{kj} - \frac{2r_j\{\boldsymbol{R}_{kj} + \boldsymbol{r}_A - [(\boldsymbol{r}_A + \boldsymbol{R}_{kj}) \cdot \boldsymbol{n}_j]\boldsymbol{n}_j\}}{\sqrt{(\boldsymbol{R}_{kj} + \boldsymbol{r}_A)^2 - [(\boldsymbol{R}_{kj} + \boldsymbol{r}_A) \cdot \boldsymbol{n}_j]^2}} \right\} \cdot \mathrm{d}\boldsymbol{r}_A \tag{5}$$

As described in Figure 3, we use angle ϕ to express $\boldsymbol{r}_A$ on the circumference of k-th disc. On k-th disc we set x' and y' as

$$x' = -\mathrm{sgn}((\boldsymbol{n}_j \times \boldsymbol{n}_k) \cdot \boldsymbol{R}_{kj}) \frac{\boldsymbol{n}_j \times \boldsymbol{n}_k}{|\boldsymbol{n}_j \times \boldsymbol{n}_k|}, \tag{6}$$

$$y' = \boldsymbol{n}_k \times \boldsymbol{x}', \tag{7}$$

where $\mathrm{sgn}(t) = 1$ for $\mathrm{t} \geq 0$ and $\mathrm{sgn}\ (t) = -1$ for $\mathrm{t} < 0$. The $\boldsymbol{x}', \boldsymbol{y}'$ and $\boldsymbol{n}_k$ make an orthogonal coordinate set. The ϕ is an angle made by $\boldsymbol{r}_A$

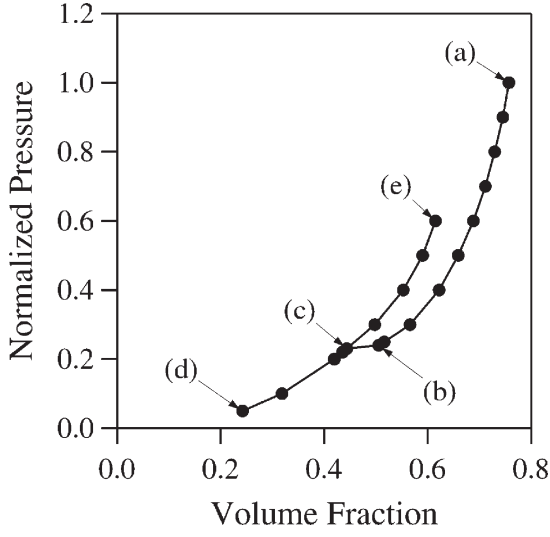

FIGURE 4 Equation of state of spherical discs of $D/L = 5$. Pressures of points indicated by arrows are (a) $p^* = 1.0$, (b) $p^* = 0.24$, (c) $p^* = 0.23$, (d) $p^* = 0.05$, and (e) $p^* = 0.6$.

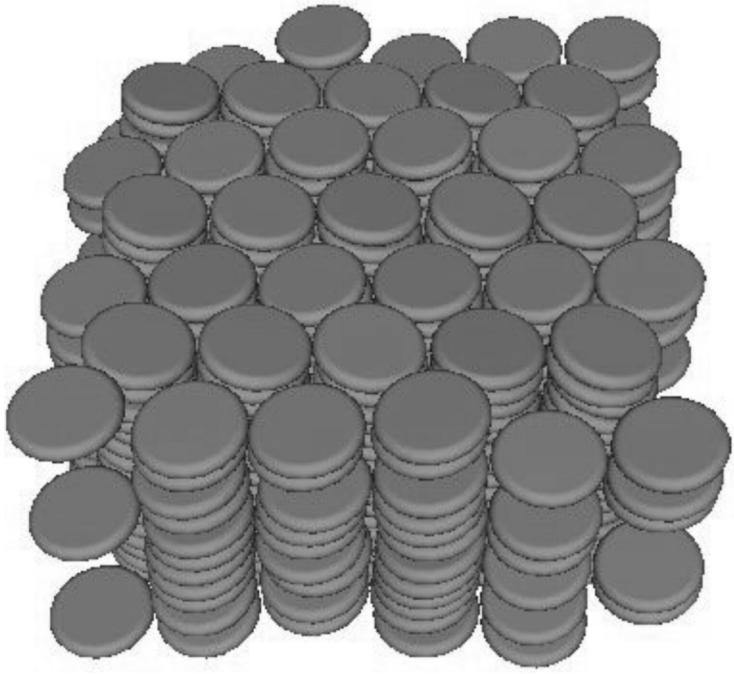

FIGURE 5 A snapshot of the system at point (a) of Figure 4.

and $\boldsymbol{y}'$. In this case we have

$$d\boldsymbol{r}_A = (\boldsymbol{r}_A \times \boldsymbol{n}_k)d\phi. \tag{8}$$

Equations (5) and (8) give

$$\frac{d\xi}{d\phi} = \left\{ 2\boldsymbol{R}_{kj} - \frac{2r_j\{\boldsymbol{R}_{kj} + \boldsymbol{r}_A - [(\boldsymbol{r}_A + \boldsymbol{R}_{kj}) \cdot \boldsymbol{n}_j]\boldsymbol{n}_j\}}{\sqrt{(\boldsymbol{R}_{kj} + \boldsymbol{r}_A)^2 - [(\boldsymbol{R}_{kj} + \boldsymbol{r}_A) \cdot \boldsymbol{n}_j]^2}} \right\} \cdot (\boldsymbol{r}_A \times \boldsymbol{n}_k) \cdot \tag{9}$$

To find the minimum distance between j-th and k-th core discs in configuration (c) of Figure 2 is equivalent to find the minimum of ξ as a function of ϕ.

Our numerical search selected global minimum from local minimums found with the help of Eq. (9). We are sure that our program generated numerical error when slight different two minimums were located closely. In that case, depending on accuracy of search, the program considered two minimums as one and returned a minimum that was slightly larger than actual minimum.

FIGURE 6 A snapshot of the system at point (b) of Figure 6.

III. SIMULATION

We performed isobaric MC simulation for a system of 480 spherical discs of $D/L = 5$. Simulation box size along x-, y-, and z-directions fluctuated for given pressure, while angles made by edges of simulation box were kept rectangular. We denote a normalized pressure by p^* that is defined as

$$p^* = pL^3/(k_B T), \tag{10}$$

where p is actual pressure, T temperature, and k_B is Boltzmann's constant.

For a given pressure, except for $P^* = 1.0$, simulation started with an initial configuration that was an equilibrium configuration at higher or lower pressure. For $p^* = 1.0$, simulation started with a closed packed structure.

Acceptance ratio was kept between 0.3 and 0.6 for trial movements of molecular configurations and system size changes. After equilibration,

we calculated average of system volume to obtain volume fraction $\eta = \upsilon_0 N/V$ of the system, where V is system volume, and N the number of spherical discs.

IV. RESULTS

Figure 4 shows relation between normalized pressure p^* and volume fraction. Figures 5–9 show snapshots of corresponding points in Figure 4. There are two branches of equation of state. One branch is of configurations that contain orders in orientation and position. Points between (a) and (b) in Figure 4 belong to this branch. The other is of disordered configurations to which (d), (c), and (e) of Figure 4 belong. In the pressure decreasing process, where initial configuration of a simulation run for a given pressure was an equilibrium configuration at higher pressure, transition from ordered branch to disordered branch was between points (b) and (c) of Figure 4.

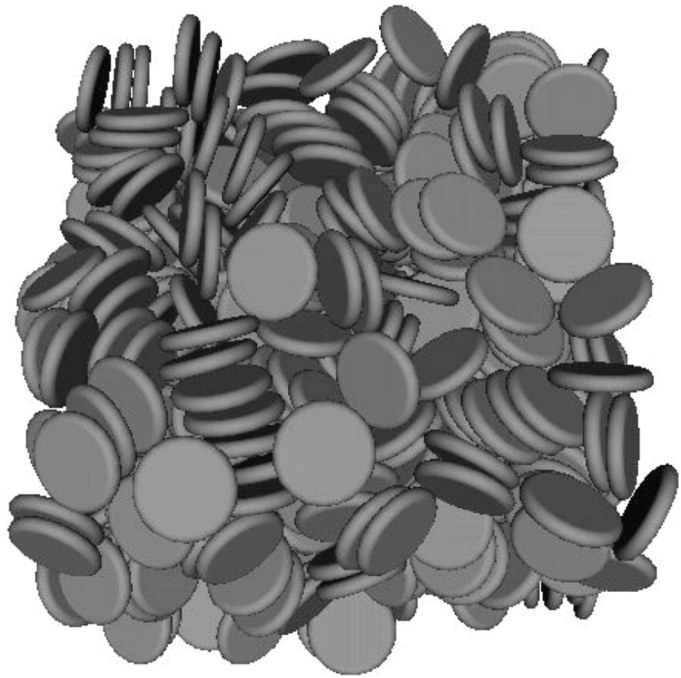

FIGURE 7 A snapshot of the system at point (c) of Figure 7.

V. CONCLUDING REMARKS

In the present stage, we have not examined detail of positional correlation to classify ordered configurations into crystal or columnar phase. When we decreased pressure, ordered state of hexagonal columns of spherical discs melted into disordered state without showing nematic phase.

Figure 8 obviously indicates positional and orientational disorder for the point (d) of Figure 4. However in Figure 7 that belongs to disordered branch in Figure 4, local alignment order of discs exists.

As Figure 9 shows, this local column-like order grew when we increased pressure along the disorder branch of equation of state. Similar structure was reported for cut spheres by Allen and Wilson [6] as cubic structure.

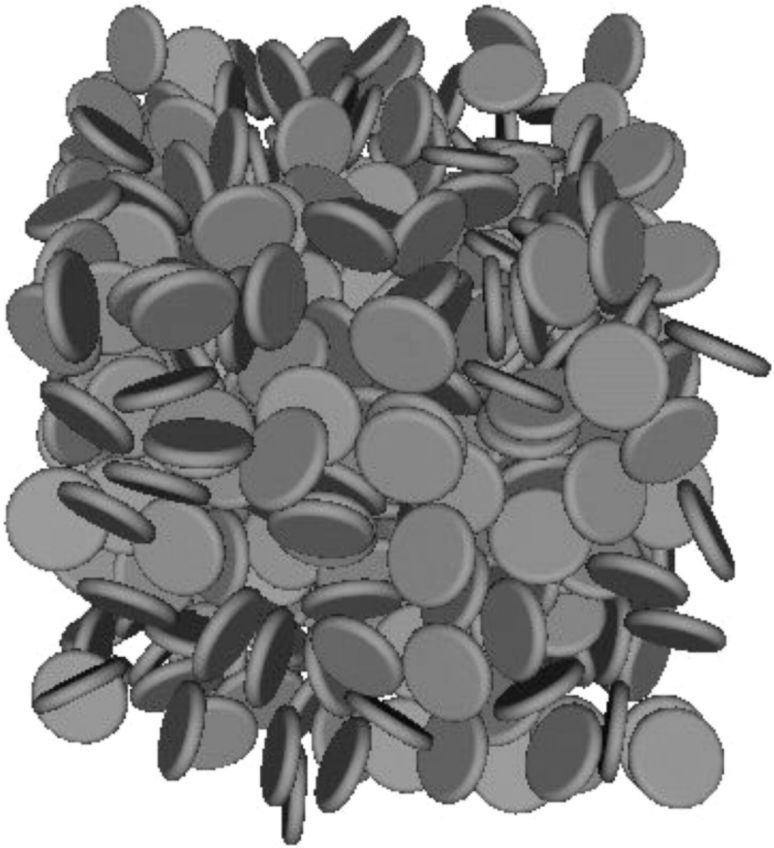

FIGURE 8 A snapshot of the system at point (d) of Figure 8.

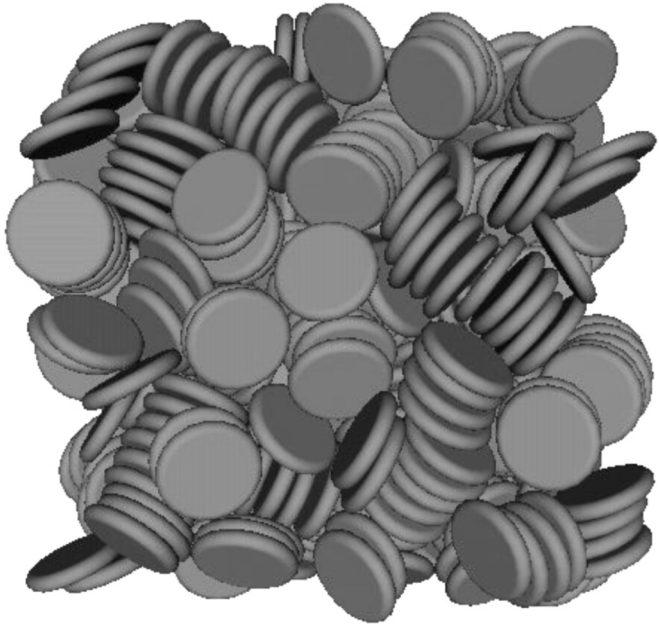

FIGURE 9 A snapshot of the system at point (e) of Figure 9.

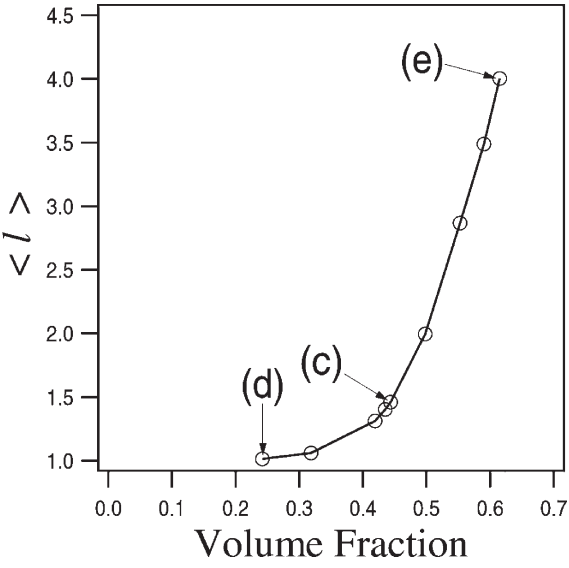

FIGURE 10 Dependence of number average of column size on volume fraction. Arrows indicate points referring Figure 4.

In the present study, we introduced a criterion that j-th and k-th spherical discs are grouped into a column when they satisfied conditions

$$\sqrt{H(|\boldsymbol{R}_{kj}|^2 - (\zeta D)^2)} < |\boldsymbol{n}_j \cdot \boldsymbol{R}_{kj}| < \sigma L, \tag{11}$$

$$\sqrt{H(|\boldsymbol{R}_{kj}|^2 - (\zeta D)^2)} < |\boldsymbol{n}_j \cdot \boldsymbol{R}_{kj}| < \sigma L, \tag{12}$$

where we used parameters $\zeta = 0.3$ and $\sigma = 1.7$ in the present case, and $H(x) = 0$ for $\mathrm{x} \leq 0$ and $H(x) = x$ for $x > 0$. We denote number of discs that is grouped into j-th column by l_j, that expresses size of the column. We consider that a single disc corresponds to a column of size 1.

We calculated $< l >$ that is an average of column size as

$$< l >= \frac{1}{M} \sum_{j=1}^{M} l_j = \frac{N}{M}, \tag{13}$$

where M is number of columns grouped in the system.

Figure 10 shows dependence of $< l >$ on volume fraction. As Figure 10 indicates, the minimum of $< l >$ is 1 given by dilute limit where all columns are made of a single disc. One of our interests was phase transition behavior of column formation in isotropic structure. Figure 10 indicates no critical behavior. We expects that local column structure continuously grows in global isotropic structure.

Figure 4 shows hysteresis of equation of state between ordered and disordered states. Calculation and comparison of free energies of these states to determine transition points is our future task.

REFERENCES

[1] Stroobants, A., Lekkerkerker, H. N. W., & Frenkel, D. (1987). *Phys. Rev*., A *36*, 2929.
[2] Veerman, J. A. C. & Frenkel, D. (1991). *Phys. Rev*., A *43*, 4334.
[3] McGrother, S. C., Williamson, D. C., & Jackson, G. (1996). *J. Chem. Phys*., *104*, 6755.
[4] Bolhuis, P. & Frenkel, D. (1997). *J. Chem. Phys*., *106*, 666.
[5] Frenkel, D. (1989). *Liq. Cryst*., *5*, 929.
[6] Allen, M. P. & Wilson, M. R. (1989). *J. Comput.-Aided Mol. Design*, *3*, 335.
[7] Frenkel, D. Mulder, B. M., & McTague, J. P. (1984). *Phys. Rev. Lett*., *52*, 287.
[8] Wojcik, M. & Gubbins, K. E. (1984). *Mol. Phys*., *53*, 397.